

# Fundamental parameters of six neglected old open clusters

Giovanni Carraro,<sup>1,2★†</sup> Annapurni Subramaniam<sup>3★</sup> and Kenneth A. Janes<sup>4★</sup>

<sup>1</sup>*Departamento de Astronomía, Universidad de Chile, Casilla 36-D, Santiago, Chile*

<sup>2</sup>*Astronomy Department, Yale University, PO Box 208101, New Haven, CT 06520-8101, USA*

<sup>3</sup>*Indian Institute of Astrophysics, II Block Koramangala, Bangalore 560034, India*

<sup>4</sup>*Department of Astronomy, Boston University, 725 Commonwealth Avenue, Boston, MA 02215, USA*

Accepted 2006 June 28. Received 2006 June 27; in original form 2006 May 24

## ABSTRACT

In this paper, we present the first *BVI* CCD photometry of six overlooked old open clusters (Berkeley 44, NGC 6827, Berkeley 52, Berkeley 56, Skiff 1 and Berkeley 5) and derive estimates of their fundamental parameters by using isochrones from the Padova library. We found that all the clusters are older than the Hyades, with ages ranging from 0.8 Gyr (NGC 6827 and Berkeley 5) to 4.0 Gyr (Berkeley 56). The latter is one of the old open clusters with the largest heliocentric distance.

In the field of Skiff 1, we recognize a faint blue main sequence identical to the one found in the background of open clusters in the second and third Galactic quadrant, and routinely attributed to the Canis Major accretion event. We use the synthetic colour–magnitude diagram method and a Galactic model to show that this population can be easily interpreted as a thick disc and halo population towards Skiff 1. We finally revise the age distribution of the old open clusters, showing that the previously suggested peak at 5 Gyr loses importance as additional old clusters are discovered.

**Key words:** open clusters and associations: individual: Berkeley 44 – open clusters and associations: individual: NGC 6827 – open clusters and associations: individual: Berkeley 52 – open clusters and associations: individual: Berkeley 56 – open clusters and associations: individual: Skiff 1 – open clusters and associations: individual: Berkeley 5.

## 1 INTRODUCTION

The present day age distribution of open star clusters in the Galactic disc is the result of two competing processes: the star formation history of the Galactic disc and the dissolution rate of star clusters (de la Fuente Marcos & de la Fuente Marcos 2004).

The dissolution of star clusters is particularly important for older clusters, the typical open cluster lifetime being of the order of 200 Myr (Wielen 1971). This way of tracing back the cluster formation history in the Galactic disc is a challenging task. Recent compilations (Friel 1995; Ortolani et al. 2005) show that the age distribution of old open clusters has an e-folding shape with a possible peak at 5 Gyr. The reality of this peak is however quite difficult to assess, and indeed a more recent analysis (Carraro et al. 2005, fig. 10) shows that the inclusion of a few overlooked clusters significantly weakens the reality of this peak and illustrates the importance

of carefully hunting for old clusters before drawing definitive conclusions. The recent study of the old cluster Auner 1 (Carraro et al. 2006) with an age of 3.5 Gyr again stresses the fact that we are still missing several old clusters.

Beginning with the paper of Phelps, Janes & Montgomery (1994), several attempts have been made to enlarge the sample of studied old open clusters (Hasegawa et al. 2004; Carraro et al. 2005, and references therein).

In an attempt to further contribute to this interesting field, in this paper we present the first photometric study of six overlooked, old open clusters having  $53^\circ \leq l \leq 130^\circ$  and  $-5.2 \leq b \leq +5.6$  (see Table 1) and provide homogeneous derivation of basic parameters using the Padova (Girardi et al. 2000) family of isochrones.

These clusters are NGC 6827, Berkeley 5, 52, 44 and 56 (Setteducati & Weaver 1960), and Skiff 1 (Luginbuhl & Skiff 1990).

The plan of the paper is as follows. Section 2 describes the observation strategy and reduction technique. Section 3 deals with star counts and radius determination. The colour–magnitude diagrams (CMDs) are described in Section 4, while Section 5 illustrates the derivation of the fundamental parameters of the clusters. Section 6 concentrates on the star cluster Skiff 1. Finally, Section 7 provides a detailed discussion of the results.

\*E-mail: gcarraro@das.uchile.cl (GC); purni@iiap.res.in (AS); janek@bu.edu (KAJ)

†Andes Fellow, on leave from Dipartimento di Astronomia, Università di Padova, Vicolo Osservatorio 2, I-35122, Padova, Italy.

**Table 1.** Basic parameters of the clusters under investigation. Coordinates are for the J2000.0 equinox and have been visually redetermined by us.

| Name        | RA<br>( <sup>h</sup> <sup>m</sup> <sup>s</sup> ) | Dec.<br>( <sup>°</sup> <sup>'</sup> <sup>''</sup> ) | <i>l</i> | <i>b</i> |
|-------------|--|---|----------|----------|
| Berkeley 44 | 19 17 12   | +19:28:00   | 53°21    | +3°35    |
| NGC 6827    | 19 48 54   | +21:12:00   | 58°25    | -2°35    |
| Berkeley 52 | 20 14 18   | +28:58:00   | 67°89    | -3°13    |
| Berkeley 56 | 21 17 42   | +41:54:00   | 86°04    | -5°17    |
| Skiff 1     | 00 58 24   | +68:28:00   | 123°57   | +5°60    |
| Berkeley 5  | 01 47 48   | +62:56:00   | 129°29   | +0°76    |

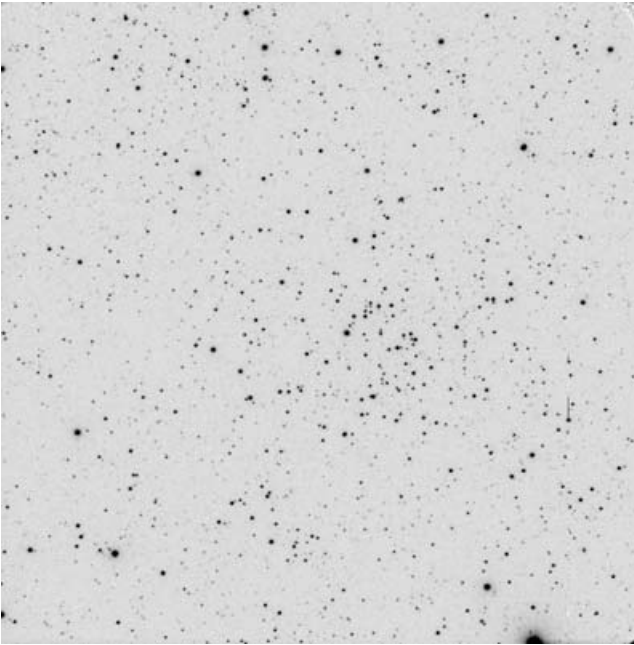


**Figure 1.** V 60-s image centred on Berkeley 44. North is up, east on the left. The field is 10 arcmin on a side.

## 2 OBSERVATIONS AND DATA REDUCTION

The observations were carried out using the 2-m Himalayan Chandra Telescope (HCT) at the Indian Astronomical Observatory (IAO), located at Hanle, India, and operated by Indian Institute of Astrophysics. Details of the telescope and the instrument are available at the Institute's home page (<http://www.iiap.res.in/>). The CCD used for imaging is a  $2k \times 4k$  CCD, where the central  $2k \times 2k$  pixels were used for imaging. The pixel size is  $15 \mu\text{m}$  with an image scale of  $0.297 \text{ arcsec pixel}^{-1}$  and the average seeing was 1.3 and 1.4 arcsec on August 9 and 30, respectively (see Table 2). The total area observed is approximately  $10 \times 10 \text{ arcmin}^2$ . Images of the clusters are presented in Figs 1–6.

The data have been reduced with the IRAF<sup>1</sup> packages CCDRED, DAOPHOT, ALLSTAR and PHOTCAL using the point spread function (PSF) method (Stetson 1987).

<sup>1</sup> IRAF is distributed by the National Optical Astronomy Observatories (NOAO), which are operated by AURA under cooperative agreement with the National Science Foundation (NSF).

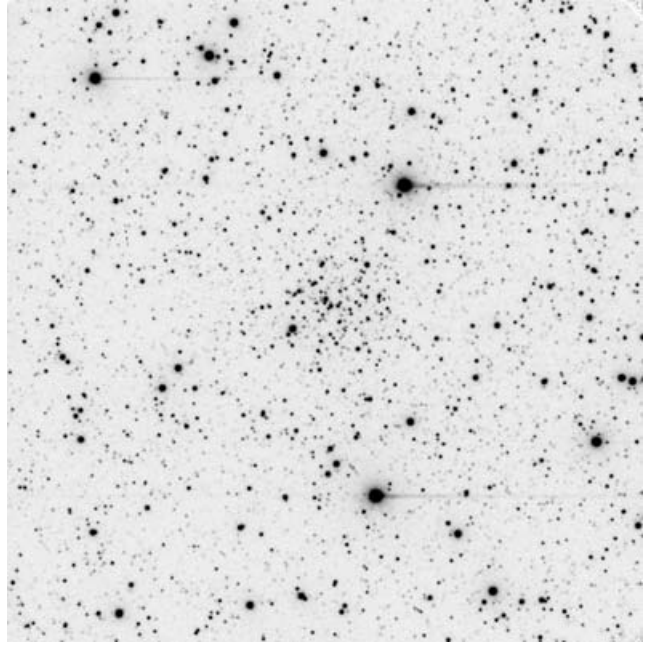


**Figure 2.** V 60-s image centred on NGC 6827. North is up, east on the left.

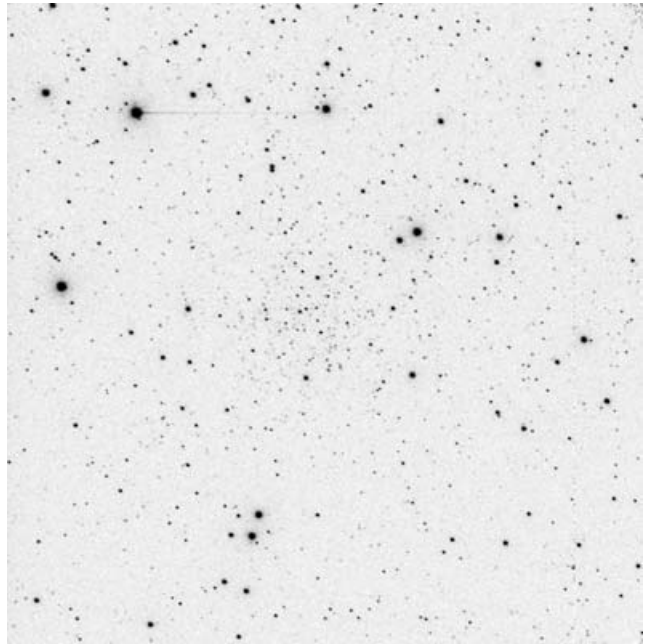


**Figure 3.** V 60-s image centred on Berkeley 52. North is up, east on the left.

The nights were photometric and the Landolt (1992) standard field SA110 was observed for calibration at different airmasses during the night to put the photometry into the standard system.

Together with the clusters, we observed two control fields, one east of Skiff 1 at RA  $01^{\text{h}}06^{\text{m}}24^{\text{s}}$ , Dec.  $+68^{\circ}29'00''$  (J2000.0), and the other north of Berkeley 44 at RA  $19^{\text{h}}17^{\text{m}}12^{\text{s}}$ , Dec.  $+19^{\circ}38'00''$  (J2000.0), to deal with field star contamination. In fact, these are the only two clusters that seem to extend beyond the field covered by the CCD.

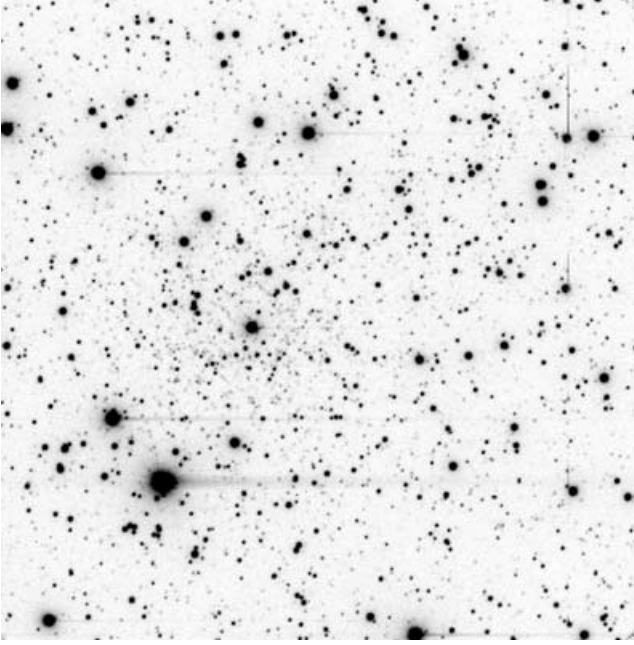


Figure 4. V 60-s image centred on Berkeley 56. North is up, east on the left.

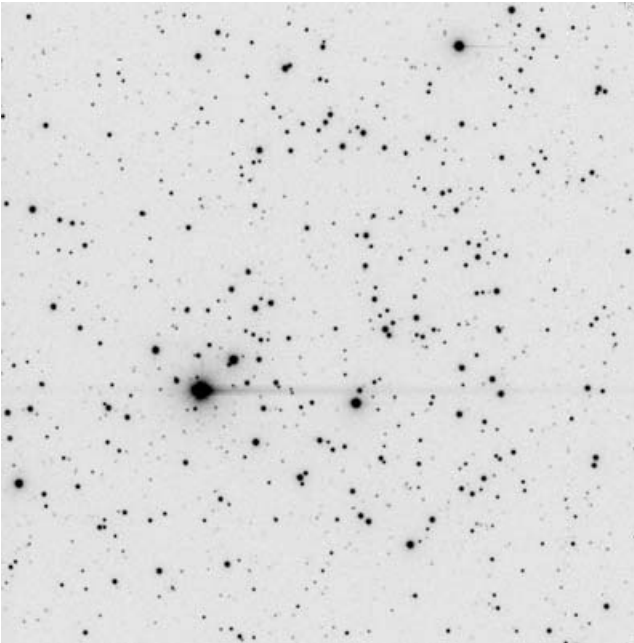


Figure 5. V 60-s image centred on Skiff 1. North is up, east on the left.

The calibration equations are of the form

$$b = B + b_1 + b_2 \times X + b_3(B - V),$$

$$v = V + v_1 + v_2 \times X + v_3(B - V),$$

$$i = I + i_1 + i_2 \times X + i_3(V - I),$$

where  $BVI$  are standard magnitudes,  $bvi$  are the instrumental ones and  $X$  is the airmass; all the coefficient values are reported in Tables 3 and 4. The standard stars in these fields provide a very good colour coverage being  $0.1 \leq (B - V) \leq 2.2$  and  $0.4 \leq (V - I) \leq 2.6$ .

Aperture correction was then derived from a sample of bright stars and applied to the photometry. We used apertures of 14 pixels for the standards stars and 7–9 pixels for the science frames, depending on

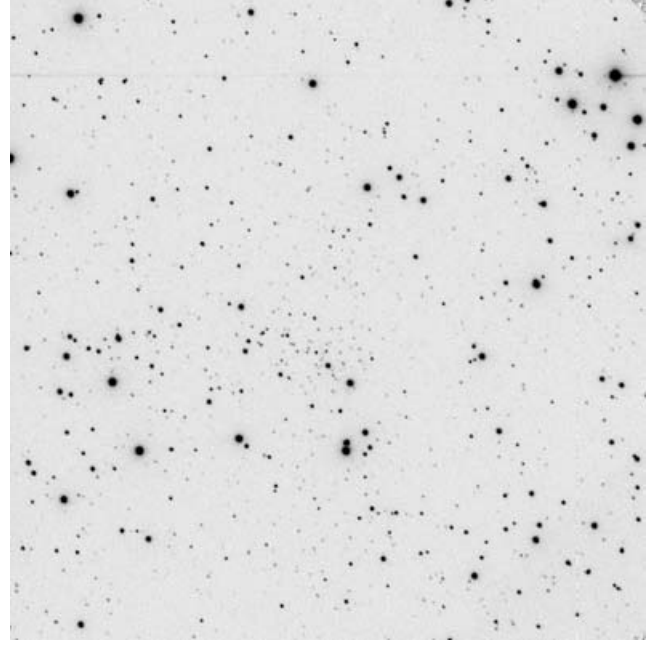


Figure 6. V 60-s image centred on Berkeley 5. North is up, east on the left.

Table 2. Log of photometric observations on 2005 August 9 and 30.

| Cluster        | Date           | Filter | Exp. time (s)            |
|----------------|----------------|--------|--------------------------|
| Be 44          | 2005 August 9  | V      | 60, 180, 2 × 300         |
|                |                | B      | 2 × 120, 2 × 600         |
|                |                | I      | 2, 5, 10, 2 × 30, 2 × 60 |
| Be 44 (field)  |                | V      | 60, 2 × 300              |
|                |                | B      | 2 × 600                  |
|                |                | I      | 2, 2 × 60                |
| NGC 6827       | 2005 August 30 | V      | 60, 180, 2 × 300         |
|                |                | B      | 120, 300, 2 × 600        |
|                |                | I      | 10, 30, 60, 2 × 120      |
| Be 52          | 2005 August 9  | V      | 60, 180, 2 × 420         |
|                |                | B      | 120, 600, 900            |
|                |                | I      | 10, 30, 120, 300         |
| Be 56          | 2005 August 30 | V      | 30, 60, 2 × 180          |
|                |                | B      | 180, 300, 600            |
|                |                | I      | 10, 30, 60, 2 × 120      |
|                |                |        |                          |
| Skiff 1        | 2005 August 30 | V      | 20, 60, 2 × 180          |
|                |                | B      | 30, 120, 300, 600        |
|                |                | I      | 10, 30, 60, 120          |
| Skiff 1 (east) |                | V      | 30, 180                  |
|                |                | B      | 60, 300                  |
|                |                | I      | 30, 120                  |
| Be 5           | 2005 August 30 | V      | 60, 3 × 180              |
|                |                | B      | 60, 300, 600             |
|                |                | I      | 10, 30, 180, 300         |

the frame. The average aperture correction amounted at 0.27, 0.29 and 0.20 mag in  $B$ ,  $V$  and  $I$ , respectively, for the night of August 9, and 0.25, 0.25 and 0.21 mag for the night of August 30.

Finally, the completeness corrections were determined by artificial-star experiments on our data. Basically, we created several artificial images by adding to the original images artificial stars. A total of approximately 4000 stars were added to the original images. In order to avoid the creation of overcrowding, in each experiment

**Table 3.** Coefficients of the calibration equations: 2005 August 9.

|                         |                       |                          |
|-------------------------|-----------------------|--------------------------|
| $b_1 = 0.803 \pm 0.007$ | $b_2 = 0.25 \pm 0.02$ | $b_3 = -0.043 \pm 0.006$ |
| $v_1 = 0.495 \pm 0.006$ | $v_2 = 0.16 \pm 0.02$ | $v_3 = 0.063 \pm 0.004$  |
| $i_1 = 0.826 \pm 0.012$ | $i_2 = 0.08 \pm 0.02$ | $i_3 = 0.044 \pm 0.009$  |

**Table 4.** Coefficients of the calibration equations: 2005 August 30.

|                         |                       |                          |
|-------------------------|-----------------------|--------------------------|
| $b_1 = 0.818 \pm 0.008$ | $b_2 = 0.26 \pm 0.02$ | $b_3 = -0.043 \pm 0.008$ |
| $v_1 = 0.513 \pm 0.005$ | $v_2 = 0.14 \pm 0.02$ | $v_3 = 0.063 \pm 0.005$  |
| $i_1 = 0.824 \pm 0.009$ | $i_2 = 0.08 \pm 0.02$ | $i_3 = 0.048 \pm 0.009$  |

we added at random positions only 15 per cent of the original number of stars. The artificial stars had the same colour and luminosity distribution as the original sample. This way we found that the completeness level stays above 50 per cent down to  $V = 20.5$ .

The limiting magnitudes are  $B = 22.0$ ,  $V = 22.5$  and  $I = 21.5$ .

The final photometric catalogues (for coordinates,  $B$ ,  $V$  and  $I$  magnitudes and errors) consist of 11 000, 10 525, 12 730, 2250, 2973, 7117 and 6486 stars for NGC 6827, NGC 6846, Berkeley 44, Berkeley 5, Berkeley 52, Berkeley 56 and Skiff 1, respectively, and are made available in electronic form at the WEBDA<sup>2</sup> site maintained by E. Paunzen.

### 3 STAR COUNTS AND CLUSTER SIZES

As a first step in the analysis of the clusters, we performed star counts to obtain an estimate of the cluster radius. This is an important step in order to pick up the most probable cluster members and minimize field star contamination. By inspecting clusters charts, we identified the cluster centre and performed star counts in circular annuli 0.5-arcmin wide around it. In order to increase the contrast, we consider in each cluster only the stars fainter than the clump.

The results are shown in Fig. 7. Here, the error bars are the Poisson error of the star counts in each annulus.

In the case of Berkeley 44 and Skiff 1, we estimate the level of the background from the accompanying offset field and draw it with a dashed line in Fig. 7.

By inspecting Fig. 7, the following considerations can be taken.

(i) NGC 6827, NGC 6846, Berkeley 52, Berkeley 56 and Berkeley 5 are compact clusters with radii between 1 and 2 arcmin.

(ii) Berkeley 44 does not show a well-defined outer radius, because star counts fall smoothly over the entire area covered by this study. For this cluster, we have observed an offset field (see Section 2), which we are going to analyse in the following section.

(iii) Although there is a visible overdensity of stars in the Skiff 1 region, the overdensity suggests the form of a ring structure 2 arcmin from the cluster nominal centre. As shown in the following discussion, Skiff 1 is both a sparse cluster and rather more nearby than the other clusters. For this reason, we have used a different annulus size (1.0 arcmin) to derive the profile.

Estimates of the cluster sizes, taken from Fig. 7, are presented in Table 5: they are in good agreement with the Dias et al. (2002) compilation, which is based on visual inspection.

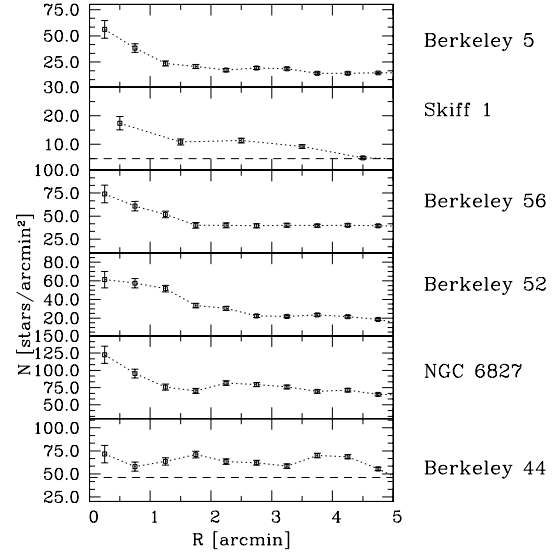


**Figure 7.** Star counts in the  $V$  passband for the clusters under investigation. The dashed lines in the Berkeley 44 and Skiff 1 panels indicate the level of the background as derived from the accompanying control field.

### 4 COLOUR-MAGNITUDE DIAGRAMS: ARE THESE REAL CLUSTERS?

By using the results of the previous section, we generate the CMDs of the clusters considering only the stars within the assumed cluster radius (Table 5). The results are shown in Figs 8 to 10. All of the clusters are located in crowded galactic plane fields and the CMDs are heavily contaminated with the projected background main-sequence (MS) population of the galaxy. In spite of this contamination, an apparent red giant clump is noticeable on all of the diagrams. We use this as our first evidence for the existence of physical clusters.

We can improve the contrast between the clusters and the background field by employing a statistical method to clean the CMDs. For each cluster, we selected a field region far from the cluster region. This selection was done in the same CCD field for all the clusters except Berkeley 44 and Skiff 1, for which we have at our disposal an offset field. The cluster and field regions have the same area.

To perform the statistical subtraction, we employed the technique described in Vallenari et al. (1992) and Gallart et al. (2003).

Briefly, for any star in the field, we look for the closest (in colour and magnitude) star in the cluster and remove this star from the cluster CMD. This procedure takes into account the photometric completeness (see Section 2).

The results are shown in the series of Figs 11 to 16. In these figures, the left panel shows the CMD for stars inside the selected radius, whereas the mid-left panel shows the offset equal area field. The *cleaned* CMD is then shown in the mid-right panel. In each case, the cleaning process leaves an apparent cluster CMD; we assume in the remainder that all of these are physical systems. Finally, the isochrone fitting is presented in the right panel (see the next section).

To get a first estimate of cluster age, we now employ the  $\Delta V$  [magnitude difference between the turn-off point (TO) and the red giant branch (RGB) clump] versus age calibration by Carraro & Chiosi (1994). This method is independent of distance and reddening, and depends only on metallicity. The results are summarized in Table 6 together with their uncertainties. The magnitude and colours of the TO have been estimated by eye, whilst the magnitude and colours

<sup>2</sup> <http://www.univie.ac.at/webda/navigation.html>

**Table 5.** Parameters of the studied clusters. The coordinate system is such that the  $Y$  axis connects the Sun to the Galactic Centre, while the  $X$  axis is positive in the direction of galactic rotation.  $Y$  is positive towards the Galactic anticentre, and  $X$  is positive in the first and second Galactic quadrants (Lynga 1982).

| Name        | Radius<br>(arcmin) | $E(B-V)$<br>(mag) | $(m-M)$<br>(mag) | $d_{\odot}$<br>(kpc) | $X_{\odot}$<br>(kpc) | $Y_{\odot}$<br>(kpc) | $Z_{\odot}$<br>(pc) | $R_{GC}$<br>(kpc) | Age<br>(Myr)   |
|-------------|--------------------|-------------------|------------------|----------------------|----------------------|----------------------|---------------------|-------------------|----------------|
| Berkeley 44 | $\geq 5.0$         | $1.40 \pm 0.10$   | $15.6 \pm 0.2$   | 1.8                  | 1.4                  | -1.1                 | 100                 | 7.6               | $1300 \pm 200$ |
| NGC 6827    | 1.5                | $1.05 \pm 0.05$   | $16.3 \pm 0.2$   | 4.1                  | 3.5                  | -2.1                 | -170                | 7.3               | $800 \pm 100$  |
| Berkeley 52 | 1.5                | $1.50 \pm 0.10$   | $18.1 \pm 0.2$   | 4.9                  | 4.5                  | -1.8                 | -270                | 8.1               | $2000 \pm 200$ |
| Berkeley 56 | 1.0                | $0.40 \pm 0.05$   | $16.6 \pm 0.2$   | 12.1                 | 12.0                 | -0.8                 | -1100               | 14.3              | $4000 \pm 400$ |
| Skiff 1     | $\geq 5.0$         | $0.85 \pm 0.05$   | $13.7 \pm 0.2$   | 1.6                  | 1.3                  | 0.9                  | 160                 | 9.5               | $1200 \pm 100$ |
| Berkeley 5  | 1.0                | $1.30 \pm 0.10$   | $18.0 \pm 0.2$   | 6.2                  | 4.8                  | 3.9                  | 80                  | 13.3              | $800 \pm 100$  |

**Table 6.** Preliminary age estimates based on the  $\Delta V$  method.

| Name        | $V_{TO}$<br>(mag) | $(B-V)_{TO}$<br>(mag) | $(V-I)_{TO}$<br>(mag) | $V_{clump}$<br>(mag) | $(B-V)_{clump}$<br>(mag) | $(V-I)_{clump}$<br>(mag) | $\Delta V$<br>(mag) | Age<br>(Gyr)   |
|-------------|-------------------|-----------------------|-----------------------|----------------------|--------------------------|--------------------------|---------------------|----------------|
| Berkeley 44 | $17.50 \pm 0.05$  | $1.75 \pm 0.10$       | $2.00 \pm 0.10$       | $16.50 \pm 0.11$     | $2.25 \pm 0.12$          | $2.50 \pm 0.14$          | $1.00 \pm 0.12$     | $1.1 \pm 0.25$ |
| NGC 6827    | $17.50 \pm 0.05$  | $1.20 \pm 0.10$       | $1.40 \pm 0.10$       | $16.75 \pm 0.25$     | $2.00 \pm 0.29$          | $2.15 \pm 0.32$          | $0.75 \pm 0.25$     | $0.8 \pm 0.20$ |
| Berkeley 52 | $20.50 \pm 0.05$  | $2.00 \pm 0.10$       | $2.20 \pm 0.10$       | $19.00 \pm 0.09$     | $2.50 \pm 0.23$          | $2.80 \pm 0.25$          | $1.50 \pm 0.10$     | $1.8 \pm 0.30$ |
| Berkeley 56 | $20.50 \pm 0.05$  | $0.80 \pm 0.10$       | $1.10 \pm 0.10$       | $17.70 \pm 0.08$     | $1.50 \pm 0.16$          | $1.75 \pm 0.18$          | $2.30 \pm 0.09$     | $4.0 \pm 0.50$ |
| Skiff 1     | $15.50 \pm 0.05$  | $1.10 \pm 0.10$       | $1.30 \pm 0.10$       | $14.70 \pm 0.11$     | $1.80 \pm 0.13$          | $2.00 \pm 0.13$          | $0.80 \pm 0.12$     | $0.9 \pm 0.20$ |
| Berkeley 5  | $19.50 \pm 0.05$  | $1.30 \pm 0.10$       | $1.50 \pm 0.10$       | $18.60 \pm 0.17$     | $2.10 \pm 0.21$          | $2.40 \pm 0.23$          | $0.90 \pm 0.18$     | $1.0 \pm 0.20$ |

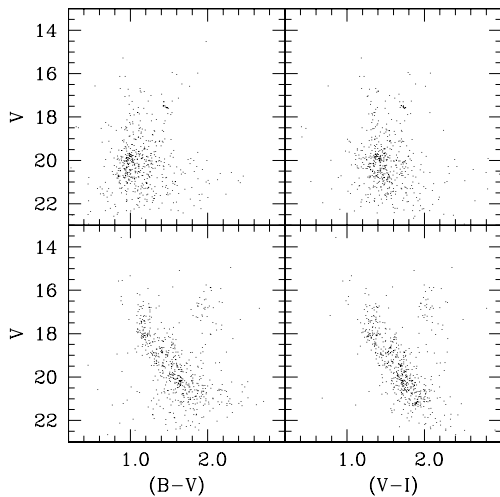


**Figure 8.** Colour-magnitude diagrams of NGC 6827 (lower panels) and Berkeley 56 (upper panels). Only the stars inside the cluster radius are shown.

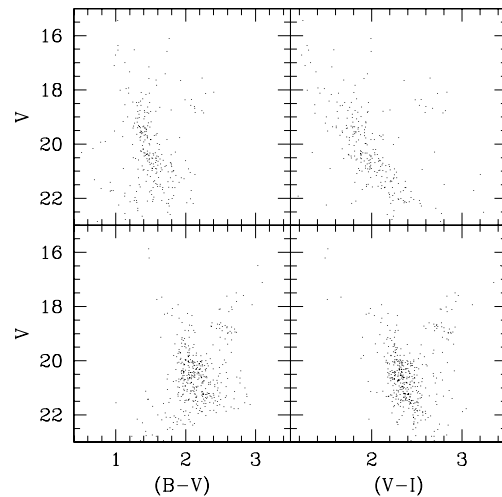


**Figure 9.** Colour-magnitude diagrams of Berkeley 52 (lower panels) and Berkeley 5 (upper panels). Only the stars inside the cluster radius are shown.

of the clump are the mean magnitude and colours of the stars in the clump area in the CMD. Based on this method, all the clusters are of Hyades age or older, with Berkeley 56 being the oldest of the sample.

An inspection of each CMD allows us to derive the following considerations.

(i) NGC 6827 looks like an intermediate-age cluster, with a prominent clump of stars at  $V \approx 16.5$  and  $(B-V) \approx 2.7$ ,  $(V-I) \approx 2.1$ . The TO is located at  $V \approx 17.75$ ,  $(B-V) \approx 1.0$ . The MS looks truncated at  $V \sim 19.5$  as a result of the cleaning procedure.

(ii) Berkeley 52 is a faint and heavily reddened cluster. The presence of a clear clump witnesses that the cluster is relatively old.

(iii) Berkeley 5 is a poorly populated cluster; the clump, if real, is very sparse, which can be a signature of significant differential reddening. The TO however is readily detectable, which ensures the reality of this cluster.

(iv) Berkeley 56 looks a promising old cluster, with a tight clump at  $V \approx 17.5$ . The TO area is at the limit of the photometry, although the TO can easily be identified at  $V \approx 20$ .

(v) Skiff 1 is a very interesting object. There is clear clump at  $V \approx 15$ , which is not visible in the control field and ensures this is a real intermediate-age/old cluster. We have to note here (both in the cluster and the offset field) the presence of a faint blue population with a TO at  $V = 19.5$ . This is similar to the one detected in the third Galactic quadrant (Bellazzini et al. 2004) and in the second Galactic quadrant (Bragaglia et al. 2006) and routinely attributed

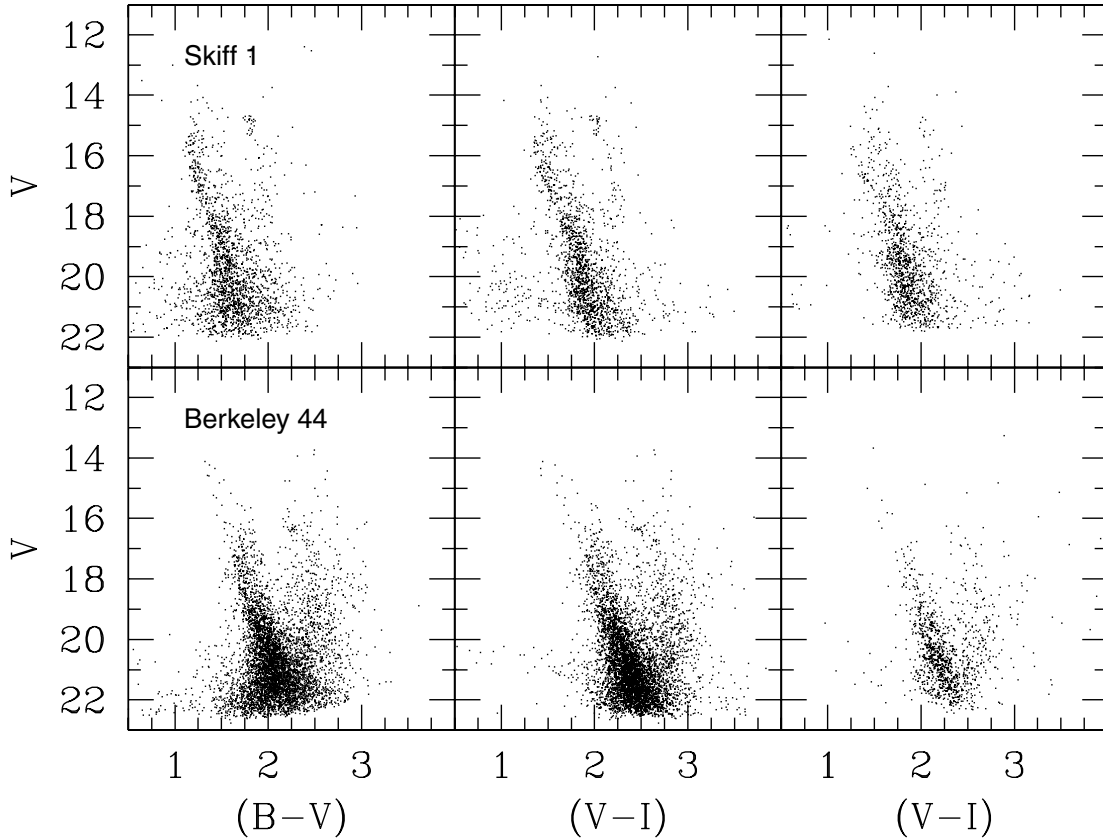


**Figure 10.** Colour–magnitude diagrams of Skiff 1 and Berkeley 44. The right panels are the comparison field. Note the anomalous blue MS with a TO at  $V = 19.5$  in the CMD of Skiff 1 and its control field.

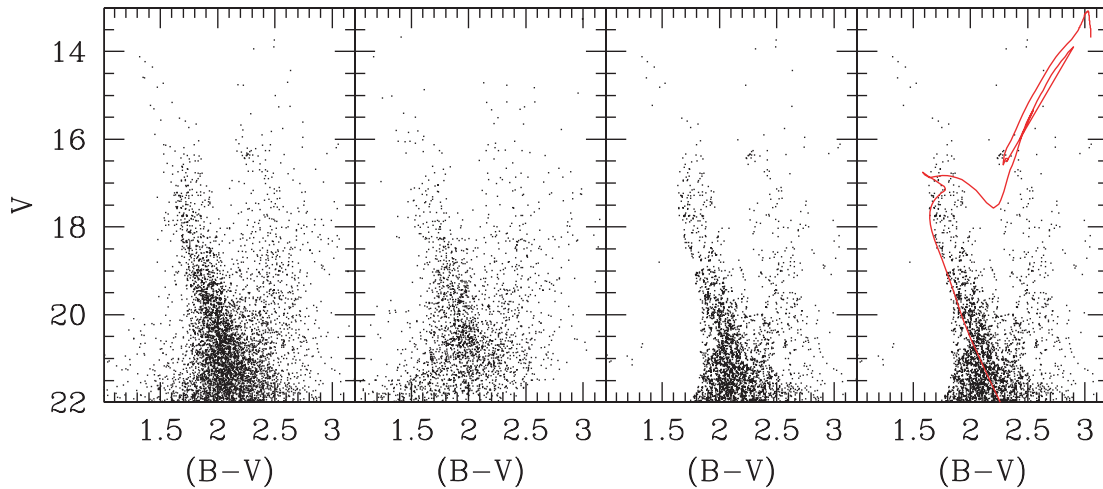


**Figure 11.** Left panel: CMD of Berkeley 44. Mid-left panel: CMD of the control field. Mid-right panel: the clean CMD. Right panel: isochrone solution for Berkeley 44; the 1.3-Gyr isochrone is shifted by  $E(B - V) = 1.40$  in  $V - M_V = 15.60$ .

to the Canis Major galaxy (Bellazzini et al. 2004). This is quite remarkable because this presumed dwarf galaxy (or its tidal tail) is not expected to extend to this galactic location (Martin et al. 2004, fig. 4).

(vi) Berkeley 44 displays severe contamination of field stars. However, the upper part of the MS and the evolved stars region are significantly more populated than in the control field. We suggest that this cluster is real.

## 5 ESTIMATES OF FUNDAMENTAL PARAMETERS

In order to derive more reliably the cluster fundamental parameters, namely reddening, age and distance, we employ the following technique, using the *cleaned* CMDs in Figs 11 to 16.

Possible isochrone solutions are obtained by exploring a large number of isochrones; for clarity only the isochrone with the best

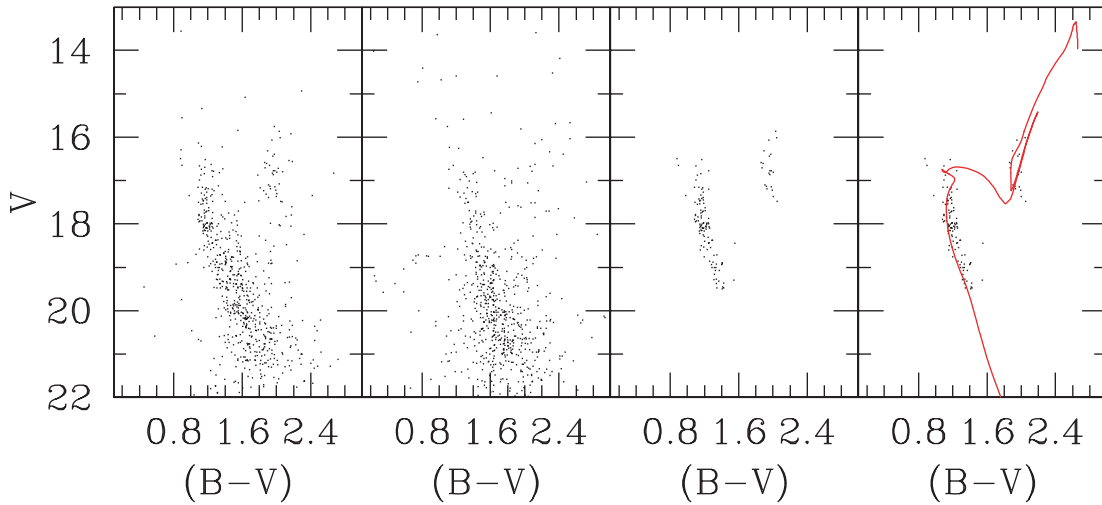


**Figure 12.** Left panel: CMD of NGC 6827. Mid-left panel: CMD of the control field. Mid-right panel: the clean CMD. Right panel: isochrone solution for NGC 6827; the 0.8-Gyr isochrone is shifted by  $E(B - V) = 1.05$  in  $V - M_V = 16.30$ .

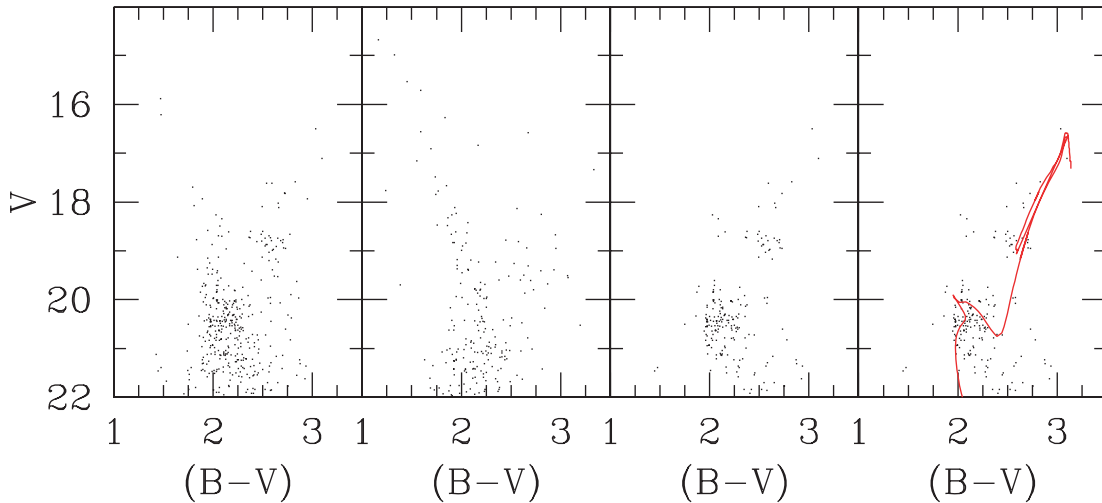


**Figure 13.** Left panel: CMD of Berkeley 52. Mid-left panel: CMD of the control field. Mid-right panel: the clean CMD. Right panel: isochrone solution for Berkeley 52; the 2.0-Gyr isochrone is shifted by  $E(B - V) = 1.50$  in  $V - M_V = 18.10$ .

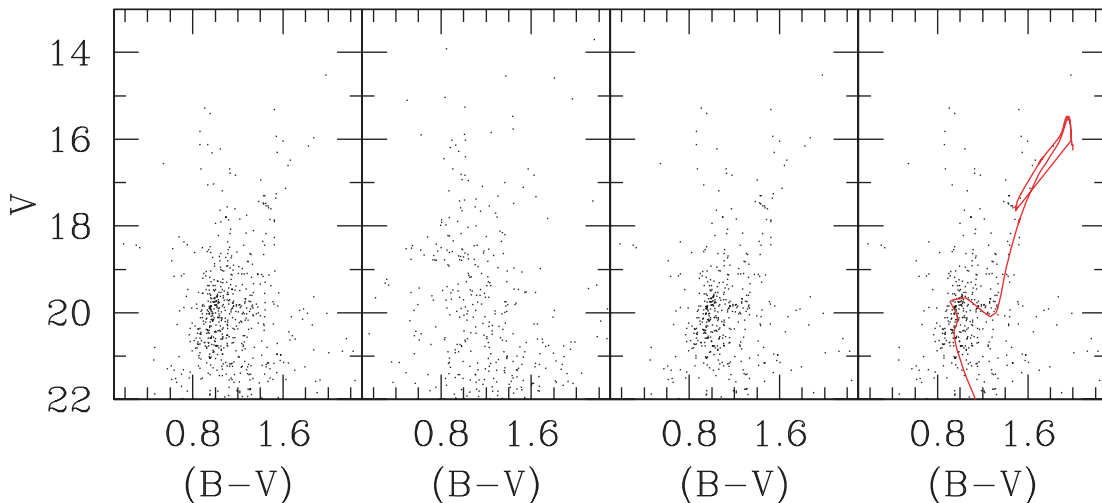


**Figure 14.** Left panel: CMD of Berkeley 56. Mid-left panel: CMD of the control field. Mid-right panel: the clean CMD. Right panel: isochrone solution for Berkeley 56; the 4.0-Gyr isochrone is shifted by  $E(B - V) = 0.40$  in  $V - M_V = 16.60$ .

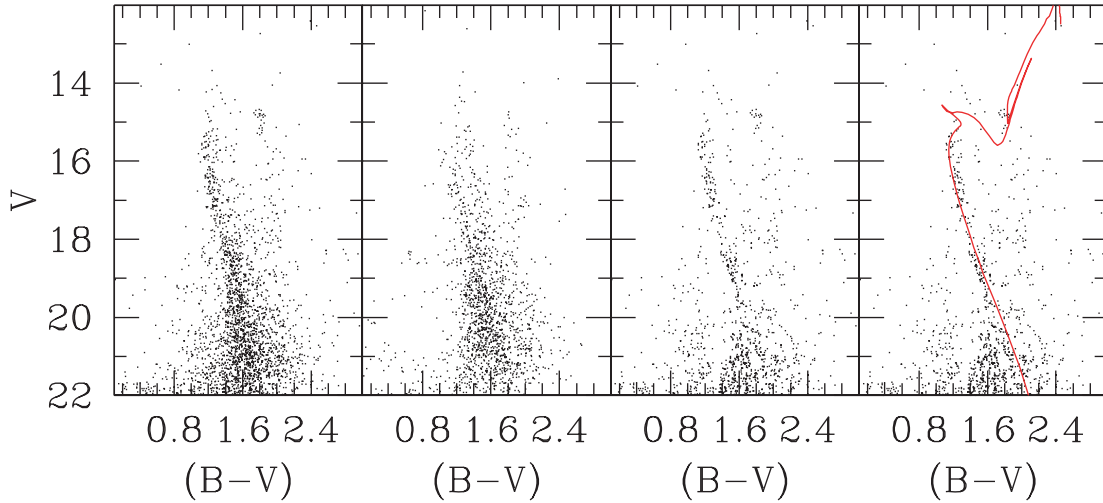


**Figure 15.** Left panel: CMD of Skiff 1. Mid-left panel: CMD of the control field. Mid-right panel: the clean CMD. Right panel: isochrone solution for Skiff 1; the 1.2-Gyr isochrone is shifted by  $E(B - V) = 0.85$  in  $V - M_V = 13.70$ .

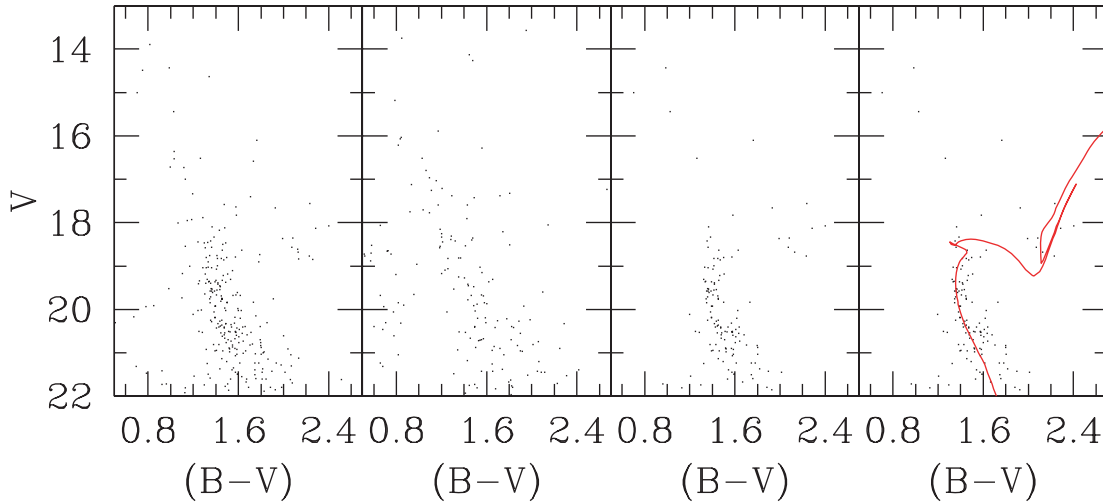


**Figure 16.** Left panel: CMD of Berkeley 5. Mid-left panel: CMD of the control field. Mid-right panel: the clean CMD. Right panel: isochrone solution for Berkeley 5; the 0.8-Gyr isochrone is shifted by  $E(B - V) = 1.30$  in  $V - M_V = 18.00$ .

visual match to the observed one is presented. To achieve the best match, we paid attention to the slope of the MS, the position and shape of the TO region, and the magnitude and colour of the RGB clump. These constraints are functions of age, metallicity, distance and reddening, and must be reproduced at the same time. Lacking a spectroscopic estimate of the metallicity, we employ the solar metallicity set.

The uncertainty in each parameter simply mirrors the degree of freedom we have in displacing an isochrone still achieving an acceptable fit.

The results of the isochrone fitting method are summarized in Table 5, where, for each cluster radius, reddening, distance modulus, heliocentric distance, Galactic Cartesian coordinates, Galactocentric distance and age are reported.

To derive the cluster heliocentric distance, we corrected the apparent distance modulus ( $V - M_V$ ) by adopting the standard ratio of selective to total absorption  $R_V = A_V / [E(B - V)] = 3.1$ .

The following few comments are in order.

(i) All the clusters are substantially reddened, with  $E(B - V)$  ranging from 0.40 to 1.50.

(ii) All the clusters are older than the Hyades, and therefore they constitute a significant contribution to the old open cluster population in the Galactic disc.

(iii) Two of them lie inside the solar circle, which is a remarkable result, because star clusters are not expected to survive so long in the dense environment typical of the inner part of the Galactic disc;

(iv) They span about 7 kpc in Galactocentric distance, but they do not seem to follow the radial abundance gradient (Carraro, Ng & Portinari 1998); this however has to be considered a preliminary result, due to the really crude estimate of the metallicity we can infer from isochrone fitting.

(v) The oldest cluster of the sample is Berkeley 56, which also lies high on the Galactic plane, and it is one of the most distant clusters from the Sun (Friel 1995).



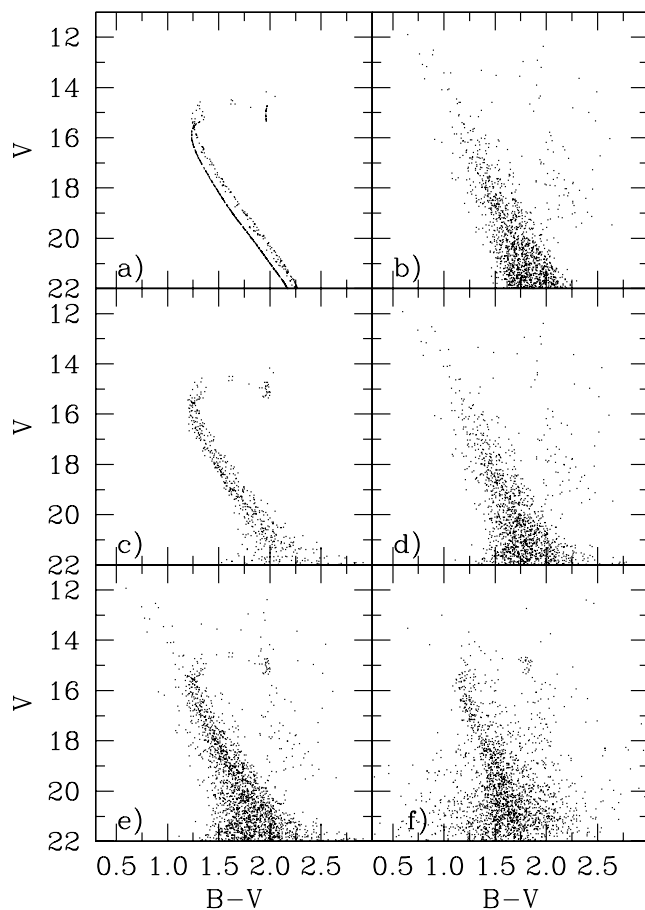


**Figure 17.** Simulation of Skiff 1 and its field in the  $V$  versus  $B - V$  diagram. (a) Simulation of a 1.2-Gyr-old cluster with  $Z = 0.019$  and an initial mass of  $1.8 \times 10^3 M_{\odot}$ , based on the same isochrones, distance modulus and colour excess as in Table 6. We have assumed that 30 per cent of the stars are binaries with mass ratios between 0.7 and 1.0. (b) Simulation of a  $10.14 \times 10.14$  arcmin<sup>2</sup> field centred at Galactic coordinates  $l = 123^{\circ}57'$ ,  $b = +5^{\circ}60'$ , performed with the Girardi et al. (2005) Galactic model. (c and d) The same as (a) and (b), respectively, after simulation of photometric errors. (e) The sum of (c) and (d), which can be compared to the observational data shown in (f).

(vi) Berkeley 56 with an age of 4 Gyr falls in an age bin where a minimum in the star cluster age distribution was suggested to exist; however, the discovery of several new clusters in this age bin (Carraro et al. 2005) significantly reduces the reality of this minimum and suggests that the age distribution of old open clusters is simply an e-folding relation.

(vii) The clean CMDs of Berkeley 44, 52 and 56 show the presence of a bunch of stars above the TO. These stars can be field stars that the cleaning procedure was not able to remove, or they can be blue stragglers and binary stars, quite common in clusters of this age.

## 6 A CLOSER LOOK AT SKIFF 1

We now concentrate a bit more on the open cluster Skiff 1. It is a nearby star cluster and, although it is not a rich cluster, among the clusters presented here, the *cleaned* CMD is the most distinct, with an MS apparently extending for more than 6 mag. This

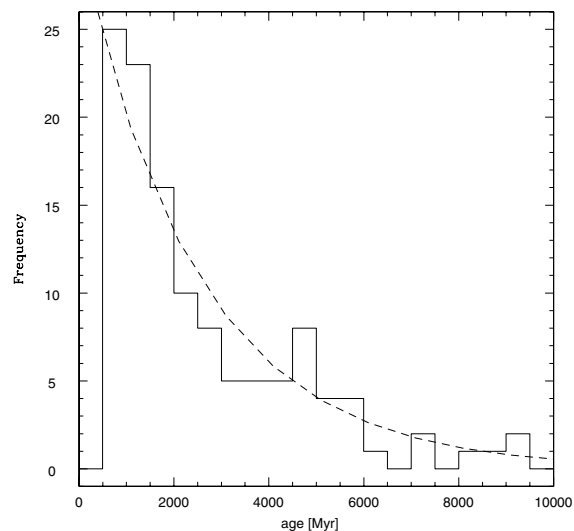


**Figure 18.** Age distribution of known open clusters older than 500 Myr. The dashed exponential line has an e-folding time of 2 Gyr.

offers the opportunity to better constrain its fundamental parameters and we employ here for this purpose the synthetic CMD technique.

The method is described in detail in Carraro, Girardi & Marigo (2002) and Girardi et al. (2005). Briefly, we count the number of clump stars ( $\sim 18$ ) and assign to the cluster a total mass ( $1.8 \times 10^3 M_{\odot}$ ) according to the Kroupa (2001) initial mass function (IMF). A population of binaries is then added, in a 30 per cent fraction, and with a mass ratio between 0.7 and 1.

Then we simulated the effect of the photometric errors, with typical values derived from our observations. The results are shown in Figs 17(a) and (c). The age, distance modulus, reddening and metallicity are the ones listed in Table 5.

In order to estimate the location of foreground and background stars, we use a Galactic model code (Girardi et al. 2005), and generate the CMD of the Galactic population in the direction of the cluster and within the same cluster area. Again, this CMD is then blurred by adding photometric errors (see Figs 17b and d).

The combination of the simulated cluster and field is then shown in Fig. 17(e), which must be compared with the observations in Fig. 17(f).

The close similarity of the simulated and observed CMDs ensures that the adopted parameters for Skiff 1 are correct within the errors and confirms the results of the simpler isochrone fitting method. Moreover, it tells us that the Galactic model successfully accounts for the field population towards the cluster. In particular, the blue MS is naturally accounted for by stars belonging to the of halo and thick disc of the Galaxy without any need to invoke an extra population.

## 7 DISCUSSIONS AND CONCLUSIONS

We have presented CCD  $BVI$  photometry for six previously unstudied possibly old open clusters, namely Berkeley 44, NGC 6827, Berkeley 52, Berkeley 56, Skiff 1 and Berkeley 5.

We have found that all the clusters are actually old and the ages range from 0.8 to 4 Gyr. This sample of clusters represents an important contribution to the poorly populated old open clusters family in the Galactic disc. In Fig. 18, we show an updated age distribution of the old open cluster (older than 500 Myr) so far known.

This comes from Carraro et al. (2005), where we added the new clusters studied in this paper and Auner 1 (3.5 Gyr; Carraro et al. 2006).

The new age distribution can be easily fitted with an exponential relation having an e-folding time of 2 Gyr. This means that, on average, the oldest clusters in the Milky Way do not survive more than 2 Gyr. This estimate is an order of magnitude larger than the typical lifetime of an open cluster (200 Myr) and suggests that old open clusters survive longer possibly due to particular situations, like birth places high on the Galactic plane, or the preferentially high total mass at birth. It might also be possible that some open clusters, especially in the anticentre, could have entered the Milky Way in the past together with cannibalized satellites (Frinchaboy et al. 2004).

Much firmer conclusions might be drawn as additional old clusters are discovered and studied.

#### ACKNOWLEDGMENTS

The work of GC is supported by *Fundación Andes*. This study made use of the Simbad and WEBDA data bases.

#### REFERENCES

- Bellazzini M., Ibata R., Martin N., Irwin M. J., Lewis G. F., 2004, *MNRAS*, 354, 1263
- Bragaglia A., Tosi M., Andreuzzi G., Marconi G., 2006, *MNRAS*, 368, 1971
- Carraro G., Chiosi C., 1994, *A&A*, 287, 761
- Carraro G., Ng K. Y., Portinari L., 1998, *MNRAS*, 296, 1045
- Carraro G., Girardi L., Marigo P., 2002, *MNRAS*, 332, 705
- Carraro G., Geisler D., Moitinho A., Baume G., Vázquez R. A., 2005, *A&A*, 442, 917
- Carraro G., Moitinho A., Zoccali M., Vázquez R. A., Baume G. 2006, *AJ*, submitted
- de la Fuente Marcos R., de la Fuente Marcos C., 2004, *New. Astron.*, 9, 475
- Dias W. S., Alessi B. S., Moitinho A., Lepine J. R. D., 2002, *A&AS*, 141, 371
- Friel E. D., 1995, *ARA&A*, 33, 381
- Frinchaboy P. M., Majewski S. R., Crane J. D., Reid I. N., Rocha-Pinto H. J., Phelps R. L., Patterson R. J., Munoz R. R., 2004, *ApJ*, 602, L21
- Gallart C. et al., 2003, *AJ*, 125, 742
- Girardi L., Bressan A., Bertelli G., Chiosi C., 2000, *A&AS*, 141, 371
- Girardi L., Groenewegen M. A. T., Hatziminaoglou E., da Costa L., 2005, *A&A*, 436, 895
- Hasegawa T., Malasan H. L., Kawakita H., Obayashi H., Kurabayashi T., Nakai T., Hyakkay M., Arimoto N., 2004, *PASJ*, 56, 295
- Kroupa P., 2001, *MNRAS*, 322, 231
- Landolt A. U., 1992, *AJ*, 104, 340
- Luginbuhl C., Skiff B., 1990, *Observing Handbook and Catalogue of Deep-Sky Objects*. Cambridge Univ. Press, Cambridge
- Lynga G., 1982, *A&A*, 109, 213
- Martin N., Ibata R., Bellazzini M., Irwin M. J., Lewis G. F., Denhen W., 2004, *MNRAS*, 348, 12
- Ortolani S., Bica E., Barbuy B., Zoccali M., 2005, *A&A*, 429, 607
- Phelps R. L., Janes K. A., Montgomery K. A., 1994, *AJ*, 107, 1079
- Setteducati A. E., Weaver M. F., 1960, *Newly Found Stellar Clusters*. Radio Observatory Lab., Berkeley
- Stetson P., 1987, *PASP*, 99, 191
- Vallenari A., Chiosi C., Bertelli G., Meylan G., Ortolani S., 1992, *AJ*, 104, 1100
- Wielen R., 1971, *A&A*, 13, 309

This paper has been typeset from a  $\text{T}_{\text{E}}\text{X}/\text{L}^{\text{A}}\text{T}_{\text{E}}\text{X}$  file prepared by the author.